

Modeling Diffusion of Adsorbed Polymer with Explicit Solvent

Tapan G. Desai and Pawel Keblinski

Department of Materials Science and Engineering, Rensselaer Polytechnic Institute, Troy, New York, USA

Sanat K. Kumar*

Department of Chemical Engineering, Columbia University, New York, New York, USA

Steve Granick

Departments of Materials Science and Engineering, Chemistry, and Physics, University of Illinois, Urbana, Illinois, USA

(Received 8 November 2006; published 21 May 2007)

Computer simulations of a polymer chain of length N strongly adsorbed at the solid-liquid interface in the presence of explicit solvent are used to delineate the factors affecting the N dependence of the polymer lateral diffusion coefficient, D_{\parallel} . We find that surface roughness has a large influence, and D_{\parallel} scales as $D_{\parallel} \sim N^{-x}$, with $x \approx 3/4$ and $x \approx 1$ for ideal smooth and corrugated surfaces, respectively. The first result is consistent with the hydrodynamics of a “particle” of radius of gyration $R_G \sim N^{\nu}$ ($\nu = 0.75$) translating parallel to a planar interface, while the second implies that the friction of the adsorbed chains dominates. These results are discussed in the context of recent measurements.

DOI: [10.1103/PhysRevLett.98.218301](https://doi.org/10.1103/PhysRevLett.98.218301)

PACS numbers: 82.35.Gh, 83.10.Rs, 83.80.Rs

While there is good understanding of polymer diffusion in unconfined solutions and melts [1,2], the same is not so for polymer dynamics at surfaces [3]. Historically, studies of unconfined diffusion began with the conceptually simple problem of an isolated chain dissolved in a sea of solvent [1,2]. In this case, hydrodynamic interactions have the effect of modifying the chain length N dependence of the translational diffusion coefficient D of the Rouse model ($D \sim N^{-1}$), which neglects hydrodynamic interactions, to $D \sim N^{-1/2}$ for ideal random walk chains. We proceed similarly and consider an isolated chain strongly adsorbed on a surface: the chain assumes a “pancake” conformation in which its size normal to the surface is of the order of a monomer size and independent of N . While the diffusion coefficient parallel to the surface scales as $D_{\parallel} \sim N^{-1}$ for DNA diffusing on phospholipid bilayers [4,5], experimental results on hard surfaces have found $D_{\parallel} \sim N^{-3/2}$ [6,7]. While the lipid results are consistent with Rouse dynamics it is unclear why hydrodynamics appear to be unimportant. Similarly, the results for the solid surfaces remain unexplained. Reasoning by analogy with what is known about unconfined polymer diffusion [8], previous workers [6] have suggested that including hydrodynamic interactions might allow us to rationalize these results. Prior simulations of surface polymer diffusion (which did not include solvent) yielded $D_{\parallel} \sim N^{-1}$ [9–12]. Our simulations include solvent molecules so as to critically study the role of hydrodynamics. Surprisingly, we find for the special case of analytically smooth surfaces that $D_{\parallel} \sim N^{-3/4}$. Surfaces with uniform friction, on the other hand, show $D_{\parallel} \sim N^{-1}$ even with explicit solvent. Our simulations then do not explain the $D_{\parallel} \sim N^{-3/2}$ result found on hard surfaces, and we speculate on other facts which might explain this scaling law.

The simulation model, i.e., a single chain dissolved in solvent, closely follows Refs. [13,14]. The solvent molecules interact with each other and polymer beads via the same potential that characterizes the interaction between any two chain monomers: specifically, we truncated the Lennard-Jones potential at its minimum and shifted it so that it is repulsive everywhere. The polymer chains are represented by the Kremer and Grest model [15,16] where N is varied from 30 to 120 in a series of simulations. The solution is confined between two walls, uniformly adsorbing to both the polymer segments and the solvent, and separated by a distance M . In the lateral direction the system is a square of size L with periodic boundary conditions. L and M varied systematically in a series of simulations. The reduced density is $\rho^* = \rho\sigma^3 = 0.74$, where ρ is the monomer number density. A velocity rescaling thermostat is used to set the temperature $k_B T/\epsilon = 1$ where k_B is Boltzmann’s constant. We use a molecular-dynamics simulation method (MD) with a time step of 0.005, where time is defined in Lennard-Jones (LJ) units. All structures for $N = 80$ are equilibrated for 3×10^6 MD steps before the data production runs, which are typically 100×10^6 steps long. Our equilibration criteria (discussed in [13]) found that the relaxation time for $N = 80$ chains is 3×10^6 MD steps. The radius of gyration parallel to the surface for the adsorbed $N = 80$ chains is $\sim 7\sigma$.

Three types of surfaces are considered. First, we modeled a smooth planar surface. As discussed in [13], we integrate over the surface and derive an effective monomer-wall potential that depends only on the distance from the surface. Note that all wall-monomer interactions (including solvent and chain monomers) are identical. The Lennard-Jones attraction was selected such that the integrated potential of about $6k_B T$ caused the polymer chains

to adsorb strongly and assume known two-dimensional conformations [13]. We conjecture that polymer adsorption occurs even though all surface-monomer interactions are identical since the distance between bonded neighbors on a chain is slightly less than the monomer size: thus, adsorbing polymer chains on the surface yields slightly more energy gain than adsorbing solvent. The second surface is similar to case (i) but is atomically corrugated. To achieve this we modify the potential $U_{\text{smooth}}(z)$ of case (i): $U(x, y, z) = U_{\text{smooth}}(z)[1 + A \cos(\frac{2\pi x}{q}) \sin(\frac{2\pi y}{q})]$, with $q = 1$ (in units of bead diameter, σ) and $A = 0.2$. The third surface is smooth but is constructed to enforce a “stick” boundary condition. Inspired by Maxwell’s idea of a “perfectly adsorbing” wall, we randomize a bead’s x - y velocity while keeping its net magnitude constant when it collides with the wall. This eliminates wall slip.

The D_{\parallel} was obtained by two independent methods whose results matched to within 5%. First, we used the Einstein equation with the mean squared in-plane displacement of the chain center of mass as a function of time. Second, we use $D_{\parallel} = \frac{1}{2} \int_0^{\infty} \langle v_{xy}(t) \cdot v_{xy}(0) \rangle dt$, where v_{xy} is a vector that only includes the x - y velocity components of the chain center of mass.

We first consider analytically smooth walls because they introduce interesting finite-size effects. In unconfined (three-dimensional) systems, finite-size effects cause D_{\parallel} to increase with system size [17]. In contrast to this expectation, we find that D_{\parallel} decreases sharply with L until $L \approx 2R_G$ [17]. We conjecture that this follows since the perpendicular component of R_G decreases with increasing L especially when $L \sim R_G$ [13]. In this range, the apparent polymer concentration near the surface is higher since the chain “sees” its own periodic images. Thus, the chain acts more bulklike and diffuses faster. Figure 1(b) shows D_{\parallel} as a function of N for fixed lateral size of the simulation cell (L) and a range of distances between the walls (M). While the slopes in this figure are not quantitative since we have only 3 points for each M , it is unambiguous that (i) D_{\parallel} increases with increasing wall separation and (ii) with increasing M the apparent D_{\parallel} depends less on N . Following [17] we plotted D_{\parallel} as a function of $1/M$. We find a well-defined $1/M \rightarrow 0$ limit for each N , but the resulting asymptotic D_{\parallel} values are independent of N . This is not physically reasonable. Thus some other effect is in play here. We postulate that these unusual finite-size effects are driven by the fact that the polymer chain resides essentially within the solvent that is immediately next to the solid wall. This layer of solvent (as a whole) displays diffusive behavior, suggesting that it is “drifting” and “entraining” the chain, even though individual solvent particles are entering and leaving the layer.

Figure 2(a) shows that the diffusivity of the center of mass of the first layer of the solvent varies as L^{-2} . This can be rationalized by considering the Langevin equation for the motion of the entire first layer of solvent: $m \frac{du}{dt} = -\Gamma u + F(t)$, where $F(t)$ is a random force, u is the layer

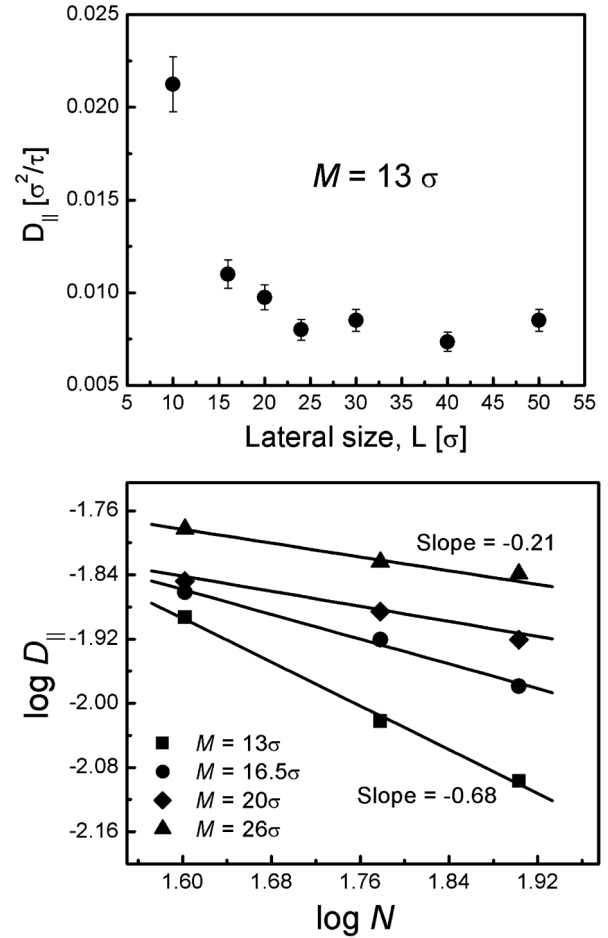


FIG. 1. Dependence of D_{\parallel} on lateral size of the simulation cell (L) and distance between walls (M) for smooth surfaces. (a) D_{\parallel} is plotted linearly against L for $M = 13\sigma$ and $N = 80$. (b) D_{\parallel} as a function of N for $L = 24\sigma$ and $M = 13, 16.5, 20, 26\sigma$.

drift velocity, m is the mass of the first layer of the solvent and Γ is the friction coefficient. The fluctuation-dissipation theorem yields, $D_{\text{solvent}\parallel} = \frac{k_B T}{\Gamma}$. Since Γ is proportional to layer area, L^2 , the observed scaling follows. Similarly, we consider $Z(t) = \langle v_{xy,c.m.}(t) \cdot v_{xy,c.m.}(0) \rangle$ where $v_{xy,c.m.}(t)$ is the velocity of the center of mass of the solvent layer. Figure 2(b) shows that, at fixed wall separation, $Z(t)/Z(0)$ is independent of L . Thus, it follows that the L dependence of the $D_{\text{solvent}\parallel}$ is only caused because $Z(0)$ depends on L . We now employ the equipartition theorem, $Z(0) = k_B T/m$, where m is the mass of the layer. Again, $D_{\text{solvent}\parallel} \sim 1/L^2$ follows. Parenthetically, we point out that for strictly 2D systems the diffusion constant should diverge as $\ln(L)$ [18]. However, this argument is not relevant here since we deal with a three-dimensional system, and we merely consider the in-plane diffusion of a single layer of solvent.

Now we discuss how the first layer diffusivity depends on wall separation, M . Above, we showed that $Z(0)$ only depends on L . Thus, the observed M dependence of solvent diffusivity implies that the relaxation time changes with M

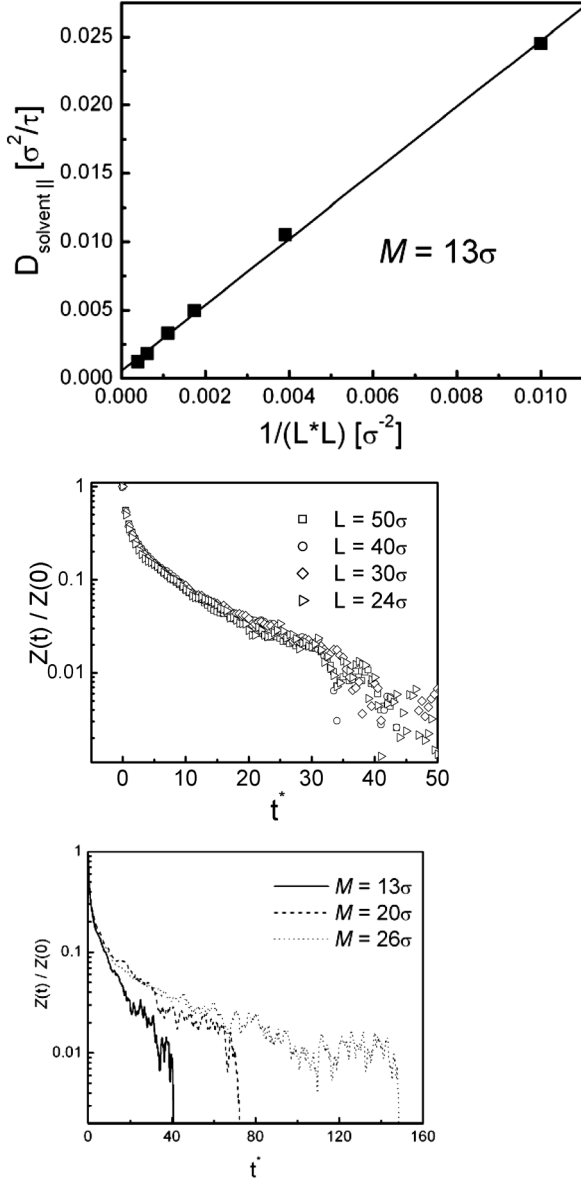


FIG. 2. Analysis of near-surface solvent diffusion for smooth surfaces. (a) $D_{\text{solvent}||}$ is plotted against $1/L^2$. (b) $Z(t)/Z(0)$ vs time for $M = 13\sigma$ and for L values as indicated (c) $Z(t)/Z(0)$ vs time for $L = 13\sigma$ and for M values as indicated.

[Fig. 2(c)]. It is apparent that the relaxation time for $M = 26$ is about 4 times larger than for $M = 13$. Thus, doubling M requires quadrupling the time needed for a shear viscous signal to propagate through the medium [19]. (Shear waves enter because polymer chains sustain Brownian diffusion in explicit solvent: thus, even though the system is quiescent, there are instantaneous shear fields.) We have explored the generality of these observations and find that this finite-size effect is observed, but is much smaller, for corrugated and nonslip walls. In the thermodynamic limit ($L \rightarrow \infty$), the diffusivity of the first layer of the solvent must approach zero. To remove this finite-size effect we calculate the diffusion of the center of mass of the polymer chain *relative* to the center of mass of the solvent layer. We

thus calculate a “mutual diffusivity”, which reduces to a self diffusivity in the thermodynamic limit: $D_{\text{mutual}||} = \frac{1}{2} \times \int_0^\infty \langle v_x^m(t)v_x^m(0) + v_y^m(t)v_y^m(0) \rangle dt$, where the index m refers to the velocity of the polymer chain with respect to the first layer of the solvent [e.g., $v_x^m(t) = v_x^{\text{polymer}}(t) - v_x^{\text{solvent layer}}(t)$].

Figure 3(a) shows that applying this finite-size correction causes all of our findings for various L and M values to superpose onto essentially a single curve. We find: $D_{\text{mutual}||} \sim N^{-x}$ with $x = 0.75 \pm 0.05$. To test this power-law dependence and the finite-size correction procedure on which it is predicated, we calculated the relaxation time of the polymer end-to-end distance vector, τ_{smooth} , and the radius of gyration, $R_{G||}$. Figure 3(c) shows that $\tau_{\text{smooth}} \sim N^{2.25}$. Since $D_{||} \sim R_{G||}^2/\tau$, $x = 0.75$ is recovered from this independent analysis. It is interesting that, while this value agrees with what one would expect from the Stokes-Einstein formula, $D_{||} \sim 1/R_{G||}$ (where $R_{G||} \sim N^{0.75}$ for adsorbed chains), it differs from that obtained in simulations of polymer diffusion on a smooth surface *without* explicit solvent, i.e., $D_{||} \sim N^{-1}$ [9–12]. The difference probably arises since the Monte Carlo simulations without solvent implicitly assume that adsorbed chain segments experience independent friction. Apparently, the inclusion of explicit solvent changes the scaling prediction.

The mutual diffusion on corrugated and nonslip walls was also calculated; we find $x = 1$ for both cases [Fig. 3(b)]. Consistent with these ideas, $\tau_{\text{rough}} \sim N^{2.5}$ [Fig. 3(c)], from which the $x = 1$ can be independently derived. By way of perspective, this distinction between values of x has an interesting counterpart in studies of unconfined polymer diffusion, where the case of strong hydrodynamic interaction has been called “Zimm dynamics” and that of screened hydrodynamic interaction has been called “Rouse dynamics” [1,2]. In the present systems, it appears that, while on smooth walls the diffusion of polymer chain follows the Stokes-Einstein equation, surface corrugation or a no-slip boundary condition leads to a dominance of surface friction.

We conclude with a tentative comparison to experiments. The first experimental study of the N dependence of adsorbed polymer chain diffusion was for DNA diffusing on cationic phospholipid bilayers in the fluid phase [3,4]. It is readily apparent that their finding of $D_{||} \sim N^{-1}$ parallels our prediction for a no-slip or corrugated surface and explicit solvent. On physical grounds, we can rationalize this in two ways. First, the surfaces possess texture due to the underlying lipid molecules. Second, it may be expected that each (mobile) lipid molecule serves to randomize the friction experienced by the adsorbed DNA. We are aware of only one later experimental study on hard surfaces which found $D_{||} \sim N^{-3/2}$, i.e., more strongly with N [6,7]. The models presented in this manuscript do not reproduce this $x = 3/2$ scaling, thus suggesting that hydrodynamics or uniform surface friction may not be the es-

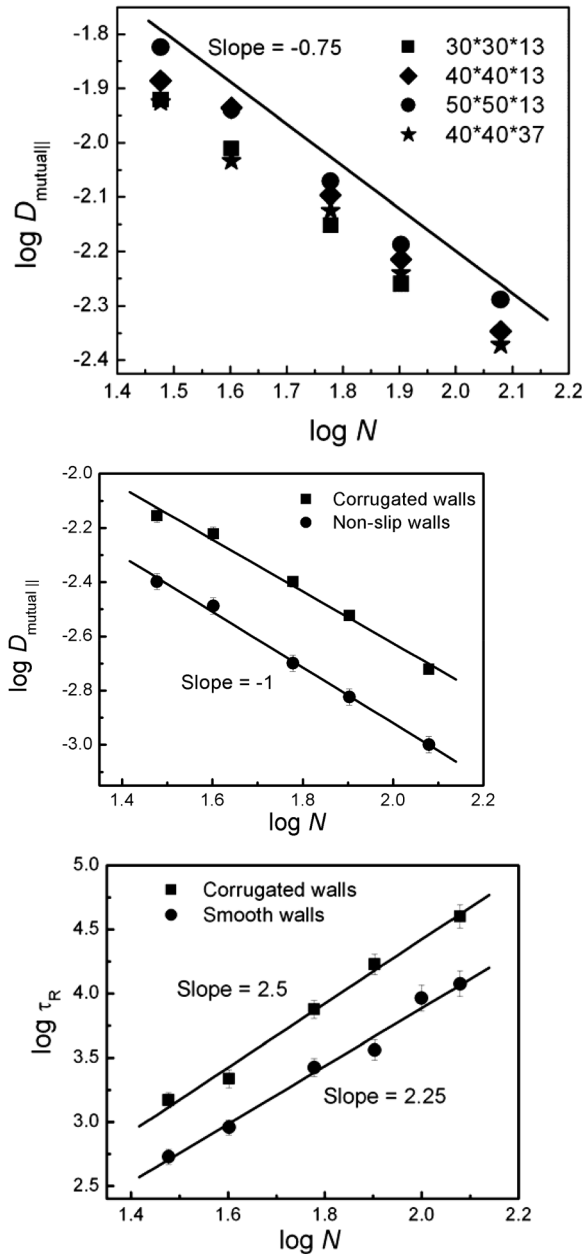


FIG. 3. $D_{\text{mutual}||}$ plotted vs N . (a) smooth surfaces. The data are consistent with the power-law slope -0.75 . The symbols refer to different system sizes as noted in the figure: the first two numbers are L and the last M . (b) Same as (a) except that the surfaces are corrugated (squares) or smooth with no-slip imposed by a Maxwell demon (circles). Lines through the points are drawn with power-law slope -1.0 . (c) Same as (b) except that the relaxation time of the polymer chain is plotted.

sential physics in these situations. However, our previous work on purely two-dimensional systems without solvent had found the $x = 3/2$ scaling when there were nonadsorbing patches with a spacing smaller than $R_{G||}$ [6,13]. In future work we plan to check if this scenario extends to surfaces with attractive patches in full three-dimensional

simulations. We shall also consider the suggestion in Refs. [6,8] that this scaling arises from lubrication force interactions between the chain as whole and the substrate for weakly adsorbed chains that do not have a simple pancake conformation.

The authors acknowledge Grzegorz Szamel (Colorado State) for the suggestion of the ‘‘Maxwell demon’’ wall. We thank Jack Douglas (NIST) for many discussions on the importance of hydrodynamic interactions. This research was funded by the National Science Foundation Nanoscale Science and Engineering Center at RPI, NSF Grant No. DMR-0117792, as well as by No. NSF-DMR-0605947 (S. G.) and No. NSF-DMR-0413755 (S. K.).

*Electronic address: sk2794@columbia.edu

- [1] M. Rubinstein and R. H. Colby, *Polymer Physics* (Oxford University, New York, 2003).
- [2] M. Doi and S. F. Edwards, *Theory of Polymer Dynamics* (Clarendon, Oxford, 1986).
- [3] H. Xu, D. Shirvanyants, K. Beers, K. Katyjaszewski, M. Rubinstein, and S. S. Sheiko, *Phys. Rev. Lett.* **93**, 206103 (2004).
- [4] B. Maeir and J. O. Radler, *Phys. Rev. Lett.* **82**, 1911 (1999).
- [5] B. Maeir and J. O. Radler, *Macromolecules* **33**, 7185 (2000).
- [6] S. A. Sukhishvili, Y. Chen, and J. D. Muller *et al.*, *Macromolecules* **35**, 1776 (2002).
- [7] S. A. Sukhishvili, Y. Chen, and J. D. Muller *et al.*, *Nature (London)* **406**, 146 (2000).
- [8] J. B. Hubbard and J. F. Douglas, *Phys. Rev. E* **47**, R2983 (1993).
- [9] E. Eisenriegler, K. Kremer, and K. Binder, *J. Chem. Phys.* **77**, 6296 (1982).
- [10] A. Milchev and K. Binder, *Macromolecules* **29**, 343 (1996).
- [11] P. Y. Lai, *Phys. Rev. E* **49**, 5420 (1994).
- [12] D. Mukherji and M. H. Müser, *Phys. Rev. E* **74**, 010601 (2006).
- [13] T. G. Desai, P. Keblinski, S. K. Kumar, and S. Granick, *J. Chem. Phys.* **124**, 084904 (2006).
- [14] T. G. Desai, P. Keblinski, and S. K. Kumar, *Polymer* **47**, 722 (2006).
- [15] K. Kremer, G. S. Grest, and I. Carmesin, *Phys. Rev. Lett.* **61**, 566 (1988).
- [16] K. Kremer and G. S. Grest, *J. Chem. Phys.* **92**, 5057 (1990).
- [17] B. Dunweg and K. Kremer, *J. Chem. Phys.* **99**, 6983 (1993).
- [18] E. Falck, O. Punkkinen, I. Vattulainen, and T. Ala-Nissilä, *Phys. Rev. E* **68**, 050102(R) (2003); O. Punkkinen, E. Falck, I. Vattulainen, and T. Ala-Nissilä, *J. Chem. Phys.* **122**, 094904 (2005).
- [19] L. D. Landau and E. M. Lifshitz, *Fluid Mechanics* (Elsevier Butterworth-Heinemann, Oxford, 2005).